

Czech Technical University in Prague
Faculty of Electrical Engineering
Department of Computer Science



Master`s Thesis

THE MATHEMATICAL MODEL OF THE FUNCTIONING OF
THE THYROID GLAND

Ekaterina Fadeeva

Supervisor: **Ing. Karel Frajták, Ph.D.**

Study Program: Open Informatics
Field of Study: Software Engineering

May 22, 2020

I. Personal and study details

Student's name: **Fadeeva Ekaterina** Personal ID number: **492138**
Faculty / Institute: **Faculty of Electrical Engineering**
Department / Institute: **Department of Computer Science**
Study program: **Open Informatics**
Specialisation: **Software Engineering**

II. Master's thesis details

Master's thesis title in English:

The mathematical model of the functioning of the thyroid gland

Master's thesis title in Czech:

Matematický model funkce štítné žlázy

Guidelines:

It is planned to consider single-chamber and two-chamber models of the thyroid gland. To improve the considered models taking into account changes in the follicle diameter. The thyroid gland consists of a large number of follicles of various sizes. The size of a single follicle varies in a fairly wide range. Expected results are the construction of a model of the thyroid gland as a megasystem consisting of individual follicles. Follicles should be interconnected, while individually resizing.

Bibliography / sources:

[1] Balykina H, Kolpak E, Kotina E. Mathematical Model of Thyroid Function. Middle-East Journal of Scientific Research 19 (3): 429-433 (2014) [2] Jackson, J.L.: The shape and size of the human thyroid follicle in health and disease. Anat. Rec. 48(2), 219-239 (1931). [3] Yocom, H.B.: Histological differences in the thyroid glands from two subspecies of *Peromyscus maniculatus*. Anat. Rec. 39(1), 57-67 (1928).

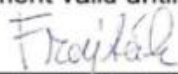
Name and workplace of master's thesis supervisor:


Ing. Karel Frajták, Ph.D., Software Testing Intelligent Lab, FEE


Name and workplace of second master's thesis supervisor or consultant:

Date of master's thesis assignment: **12.03.2020** Deadline for master's thesis submission: **22.05.2020**

Assignment valid until: **19.02.2022**


Ing. Karel Frajták, Ph.D.
Supervisor's signature


Head of department's signature


prof. Mgr. Petr Páta, Ph.D.
Dean's signature

III. Assignment receipt

The student acknowledges that the master's thesis is an individual work. The student must produce her thesis without the assistance of others, with the exception of provided consultations. Within the master's thesis, the author must state the names of consultants and include a list of references.

Date of assignment receipt

Student's signature

Acknowledgements

I would like to express my sincere gratitude for the great support and assistance in preparing my thesis Ing. Karel Frajták (CVUT), Ing. Dmitry Tumakov (KFU) and Galim Vakhitov (KFU). Especially I would like to thank my family, friends and classmates for their moral support during the whole study and writing of my thesis. I would also like to thank Arslan Enikeev, Miroslav Bureš and the entire Czech team for the opportunity to participate in the Double Degree (CVUT, KFU) program.

Declaration

I hereby declare that I have completed this thesis independently and that I have listed all the literature and publications used.

I have no objection to usage of this work in compliance with the act §60 Zákon č. 121/2000Sb. (copyright law), and with the rights connected with the copyright act including the changes in the act.

Prague, May 2020

Abstract

FADEEVA, Ekaterina: The mathematical model of the functioning of the thyroid gland.

[Master's Thesis] - Czech Technical University in Prague. Faculty of Electrical Engineering, Department of Computer Science. Supervisor: Ing. Karel Frajták, Ph.D.

The thyroid gland is an endocrine organ with the function of producing hormones that contribute to the development of the whole organism. The main exchange component is iodine. The gland itself consists of follicles - structural elements of the organ, in which the synthesized thyroid hormone accumulates in a state bound to protein.

The point-like single-chamber mathematical model of the follicle of the thyroid gland is considered. The follicle model is represented by a single camera - the combination of colloid and thyrocytes. In the proposed model, the rate of iodine exchange depends on the volume of the follicle. In turn, the volume of a colloid in the follicle depends on the concentration of treoglobulin and other molecules. Thus, in this model, the rate of exchange of iodine is made dependent on the concentration of substances in the colloid.

The thyroid gland consists of about thirty million follicles of various sizes. The size of a single follicle varies in a fairly wide range. Moreover, the size of the follicle of the thyroid gland is approximately distributed according to the normal distribution. The work of the entire thyroid gland was considered as a megasystem consisting of individual follicles having a different volume.

The mathematical model is a boundary value problem for a system of non-linear differential equations with respect to the concentrations of substances in the follicle. Calculations were carried out on graphic processors. The dynamics of changes in the size of both the individual follicle and the system as a whole under different initial and external conditions are considered. The degree of influence of the follicle volume on the rate of iodine in the follicle and on the output of the thyroid hormone T4 was estimated.

Keywords: the thyroid gland, follicle, mathematical model, graphic processors

Contents

Acknowledgements.....	4
Declaration.....	6
Abstract.....	8
List of tables.....	14
Introduction.....	16
1.1 Thesis content.....	17
Chapter 1.....	18
Thyroid Physiology.....	18
1.1 Thyroid Gland.....	18
1.2 Thyroid Follicle.....	20
Chapter 2.....	23
CUDA Technology.....	23
2.1 Why CUDA?.....	23
2.2 CUDA Terminology.....	24
2.1 NVidia Graphic Card Architecture.....	25
Chapter 3.....	27
Model Overview.....	27
3.1 Model Description.....	27
3.2 Computer Characteristics.....	29
3.3 Data preparation.....	30
3.4 Euler's method.....	35
3.4.1 Results.....	36
• Express iodine.....	36
3.5 Runge-Kutta method.....	39
3.5.1 Results.....	41
• Express iodine.....	41
3.6 Comparison of methods.....	43
3.7 Withdrawal.....	45
Conclusion.....	46
Bibliography.....	46

List of figures

Fig. 1.1: Thyroid gland structure	11
Fig. 1.2: The hypothalamus-pituitary-thyroid (HPT) axis	12
Fig. 1.3: Thyroid follicle structure	13
Fig. 2.1. Thread hierarchy in CUDA	17
Fig. 2.2: Division of the initial task into a set of independently solved subtasks	18
Fig. 2.3: GeForce 8800 GT Graphic Card Architecture	19
Fig. 3.1: Diameter Generation in one kernel	25
Fig. 3.2: Diameter Generation With Separately Curand_init() Kernel	26
Fig. 3.3: Time Comparison	27
Fig. 3.4: Start Diameter	27
Fig. 3.5: Express iodine day 5	29
Fig. 3.6: Express iodine day 10	29
Fig. 3.7: Express iodine day 15	30
Fig. 3.8: Express iodine day 20	30
Fig. 3.9: Express iodine day 25	30
Fig. 3.10: Iodine deficiency day 5	31
Fig. 3.11: Iodine deficiency day 10	31
Fig. 3.12: Iodine deficiency day 15	31
Fig. 3.13: Iodine deficiency day 20	32
Fig. 3.14: Iodine deficiency day 25	32
Fig. 3.15: Express iodine day 5	34
Fig. 3.16: Express iodine day 25	34
Fig. 3.17: Iodine deficiency day 5	35
Fig. 3.18: Iodine deficiency day 25	35
Fig. 3.19: Diameter size with Euler Method	36
Fig. 3.20: Diameter size with Runge-Kutta Method	36

List of tables

Table 1.1: Follicle size of human embryo	14
Table 3.1: Characteristics of the graphic card	22
Table 3.2: Method speed	37

Introduction

The thyroid gland is a small butterfly-like organ, which is one of the internal secretion glands. It serves as a storage of iodine and produces iodine-containing hormones.

The influence of this organ on the state of the organism in vertebrates is enormous.

One of the causes of thyroid gland pathologies is iodine deficiency or excess. Even small fluctuations can lead to thyroid disease, resulting in impaired metabolic processes, which can lead to malfunctioning of the entire body, including metabolism. In case of serious deviations, the metabolism in the body is disturbed to such an extent that body temperature is not sufficiently regulated; there is insufficient hematopoiesis, which can lead to anaemia.

According to the Ministry of Health of the Russian Federation, the number of people with thyroid diseases has increased by 14% the period from 2013 to 2017: from 2037.1 to 2323.8 cases per 100,000 of the population [13, 14]. This number continues to increase.

Mathematical models of the thyroid gland allow identifying the functions that have the most affect the general condition of the entire organ, the most dangerous disorders in its work, as well as find appropriate treatment.

Today, there is a huge variety of mathematical models of the thyroid gland functioning. Most often, they describe the gland as a single whole [3].

Some of the models study changes in the size of the thyroid gland in hypothyroidism (a condition caused by long-term, persistent lack of thyroid hormones) and autoimmune thyroiditis (inflammatory disease of the thyroid gland caused by an attack of specific proteins on the functional cells of their own body) separately. For example, work [12] shows how autoimmune thyroiditis Hashimoto upset the normal functioning of the gland by slowly destroying follicle cells through complex immune mechanisms.

Some works also study the interaction between the pituitary gland and the thyroid gland [11] or study thyroid cancer [8].

There is also another approach, in which thyroid work is studied at the cellular level. However, there are almost no such models. The one example of such work is the model of Y. E. Balykina and E. P. Kolpak, "Mathematical models of thyroid follicle functioning" [2]. This work deals with basic biochemical reactions such as iodine flows to the follicle, the synthesis of thyroglobulin protein, and the production of hormones.

The paper considers a point single-chamber mathematical model of the thyroid follicle. The follicle model is represented by one chamber - the union of colloid and thyrocytes. In the proposed model the iodine exchange rate depends on the follicle size. In turn, the volume of colloid in the follicle depends on the concentration of thyroglobulin and iodine.

Thus, this paper presents a model in which the iodine metabolism rate is put in dependence on the concentration of substances in colloid. The mathematical model represents an edge problem for the system of nonlinear differential equations concerning concentrations of substances in the follicle.

1.1 Thesis content

Mathematical modelling is an important part of experimental medicine. Interest in this area is related to the simulation of the human body and the observation of drug reactions. This reduces the number of experiments on laboratory animals and also reduces the time between the discovery of a new drug and its direct application to humans.

The purpose of the master's thesis is to construct a mathematical model of the thyroid gland taking into account changes in the diameters of functional units of the organ.

A number of tasks were set before starting the work:

1. To build a model of a separate follicle taking into account the diameter.
2. To combine all follicles into a single system.
3. When using CUDA technology to accelerate the work of the program.
4. Comparative analysis of work of parallel and sequential versions of the program.

This thesis consists of introduction, theoretical and practical chapters, results and conclusions. At the end of the work a list of literature and an application where you can find the source code are presented.

Chapter 1

Thyroid Physiology

1.1 Thyroid Gland

The thyroid is one of the organs included in the endocrine gland system. This system also includes: the pituitary gland, sex glands, adrenals, etc. They are located in different places in the human body, but form a single system to control the activity of internal organs. The hormones secreted by them (the secret) get directly into the blood as well as into the tissue fluid. The thyroid gland itself is responsible for the production of thyroids, i.e. iodine-containing hormones involved in the regulation of metabolism. The organ visually resembles a butterfly, is located in the front of the neck, consists of two lobes, right and left, connective isthmus, and in some cases has a pyramidal lobe, giving up [1, 16]. The size of the gland relative to body weight is extremely small in all animals and is about 0.20% of the body weight [17].

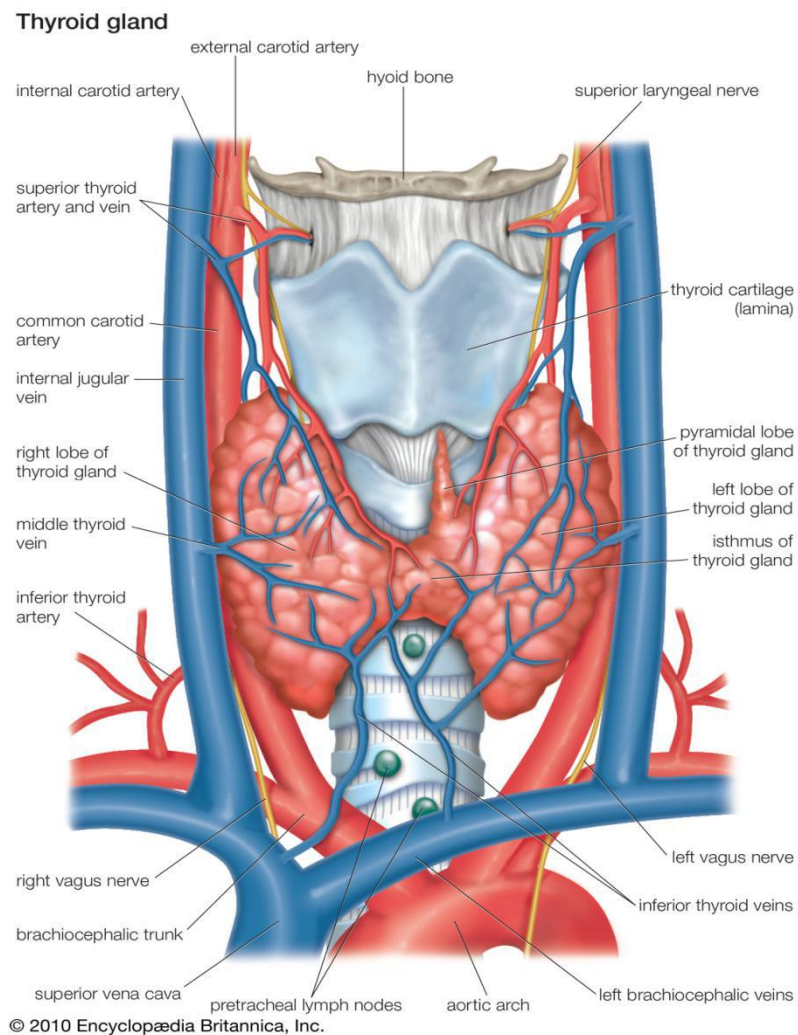


Fig. 1.1: Thyroid gland structure

The axis is a feedback system that uses hormones as signals of regulation the production and release of thyroid hormones T_3 and T_4 . In response to hormonal signals, the hypothalamus releases thyrotropin, which binds to thyroid receptors. They stimulate the synthesis and secretion of thyroid hormones [3].

Intermediate brain, which consists of two main section: the upper and lower brain, is located between the large hemispheres of the brain is the The lower section is called the Hypothalamus. The functioning of all sections of the pituitary gland is related to it. TTH hormone (thyroid hormone) secreted by the pituitary gland stimulates thyroid function.

Together they form the axis of hypothalamus-pituitary-situitary gland [3].

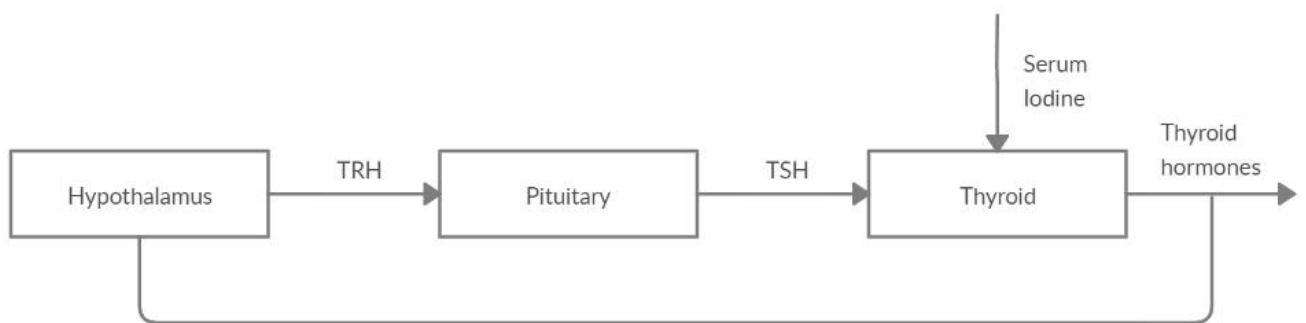


Fig. 1.2: The hypothalamus-pituitary-thyroid (HPT) axis

In the cells of the thyroid gland, follicles, hormones are stored as colloids and are released into the blood as needed. These hormones are splitting down in the kidneys and the liver. This partially covers the daily iodine requirement. The cells of the organ store a sufficient supply of hormones, at which the body may not experience iodine deficiency for up to several months. However, in the absence of iodine for a longer period of time, the hormones will not be able to produce enough.

Hypothyroidism - the so-called hypofunction of the thyroid gland, characterized by a slowdown in metabolism of all types. In children, this disease leads to stunted growth and neuropsychological development [1].

1.2 Thyroid Follicle

The main structural and functional element of the thyroid gland is the follicle. Follicles are bubbles, most often having a round or oval shape, which are filled with colloid (protein iodine-containing substance). A follicle consists of an external monolayer of follicular cells surrounding the inner nucleus and colloid, which is a storage reservoir of thyroid hormone. The colloid, stored in light, is a transparent viscous liquid. It is produced by the follicle epithelium and contains hormones produced by the thyroid gland.

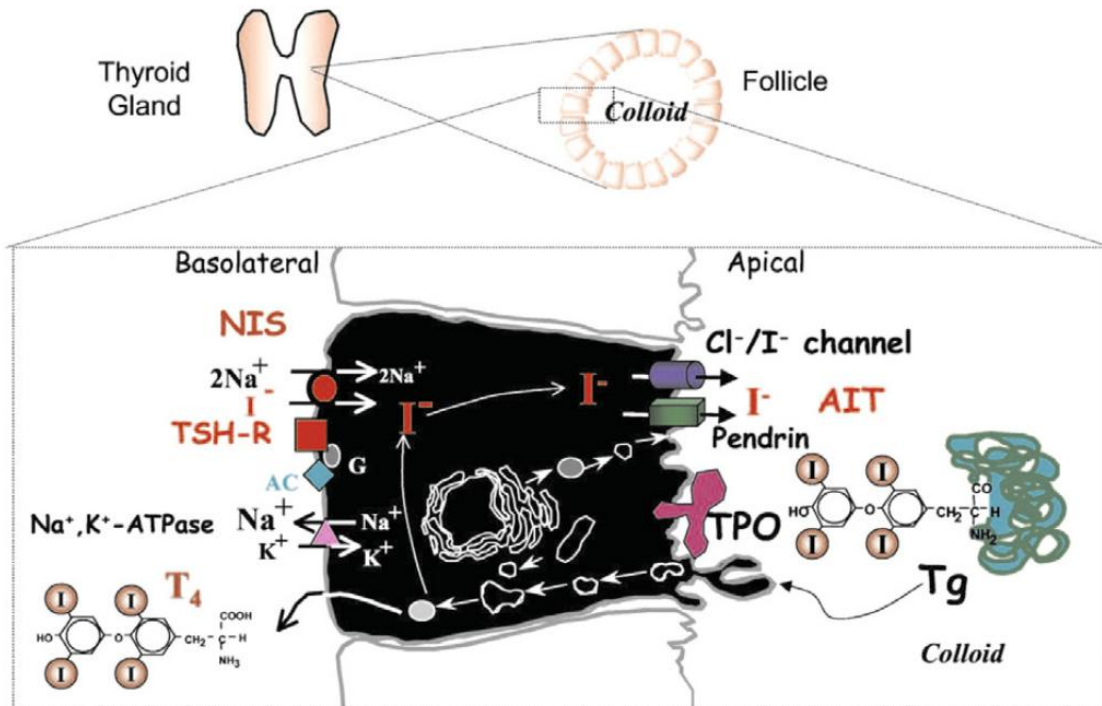


Fig. 1.3: Thyroid follicle structure

The size of the individual follicle varies a fairly wide range. The height of individual follicular cells is from 5 to 10 μm , and the diameter of the entire follicle is from 25 to 250 μm . The size of the follicles and the height of their cells vary depending on the functional state of the gland [17].

The shape of the thyroid follicle is changeable variable, but it basically has three basic types, namely, angular, round, and oval [7]. Most of the angular follicles are almond-shaped or heart-shaped, and they are rather thin when looking from the edge or in profile. Occasionally, the follicles are bizarre in shape. In some of these follicles, the bumps consist of deep clefts, and in many cases contain a small artery. There are also large diverticulums protruding from the follicle wall, which are formed when the follicle cavity is enlarged to passively place the growing amount of colloid inside [7]. However, most often researchers assume that the follicles are spherical in shape.

The size of the follicle depends on the number of cells and the number of colloids. They are interchangeable and vary depending on biological activity. Direct measurements of these variables provide information on the structures involved in the synthesis, storage and secretion of thyroid hormones, as well as changes at morphological and functional levels [5].

With some exceptions, the size of the follicle tends to increase with body size, while the epithelium percentage decreases.

The size of the thyroid follicles in mammals is roughly the same as the size of animal and the largest follicles are in humans. Note that the average follicle size increases from mouse 45.7 μm , followed by rat, cat, Guinea pig, rabbit, sheep, donkey, goat, etc. to 100 μm in a dog [7]. Then a sharp jumps in size to 170-190 microns in cattle [17], pig, camel and human.

Many researchers noted a decrease in the size of follicles from periphery to center. This was observed in muscular deer [19], hamster [6] and many other animals [10].

Below is presented the table of follicle sizes in a human embryo [9]:

Follicle sizes in different weeks of pregnancy in the human embryo		
The term of pregnancy (in weeks)	Dimensions of the central follicles (μm)	Dimensions of peripheral follicles (μm)
12	16-28	34-40
14	16-36	40-60
16	16-36	60-80
18	20-40	60-80
20	40-60	60-120
22	40-60	80-140
24	40-80	120-200
26	40-80	120-200
28	60-100	120-200
30	60-100	120-200
32	60-100	120-220
34	60-120	120-220
36	60-140	120-240

Table 1.1: Follicle size of human embryo

Thus, the follicles have the same shape for most mammals. However, the size of the follicles themselves may vary significantly depending on the size of the mammal itself. Small differences are also based by gender and age [18].

The thyroid gland consists of a large number of follicles in different sizes. The number of follicles in mammals varies widely from 40 thousand in rats [4] to 2-3 million in humans.

Chapter 2

CUDA Technology

Today, the main function of the central processing unit (CPU) is to obtain maximum performance while working with integer and floating point data, but the calculations are sequentially. What's moreover, the slowing down of calculations is due to the universality of the CPU: it requires an information-filled cache to perform its functions. However, the architecture of video card allows paralleling data processing. To speed up calculations of the built model, we decided to use CUDA (Compute Unified Device Architecture) technology - a popular technology for paralleling calculations.

This technology uses a graphics processing unit (GPU) for calculations. First introduced by NVIDIA over a decade ago, in 2007. CUDA can only work with devices manufactured by this company, but there are also similar technologies from other firms.

2.1 Why CUDA?

The performance of universal processors is mostly improved by increasing the number of cores in a single chip, whereas the increase in the frequency of the processors themselves is limited by physical capacity and high power consumption. Processors on the market tend to contain up to four cores. Moreover, they are designed for conventional applications, i.e. they use MIMD - Multiple Instruction stream, Multiple Data stream. The cores work separately, executing different instructions for different processes.

Many tasks are more profitable to run on the GPU because they are originally designed for them.

In NVidia video chips the main unit consists of about eight to ten cores, hundreds of blocks designed to perform arithmetic and logic unit (ALU) and several thousand registers. The block contains shared shared memory. Moreover, video card has global memory, to which all multiprocessors have access, local memory is present in each multiprocessor, as well as specially designed memory for storing constants.

The key factor is that these multiprocessor cores in the GPU are SIMD, i.e. one instruction is given for processing multiple data streams. Many scientific tasks require this approach to the solution. In addition, it allows to increase the number of executive blocks due to their simplification.

2.2 CUDA Terminology

- Host is a central processor (CPU).
- Device is a graphics processor (GPU) located on a graphics card.
- The kernel is a function that runs on the device.

Each processor has its own separate memory. The memory of the device and the host are physically separated. The computing processor is controlled by the host -functions for data exchange are called and tasks are launched on device from the host или host calls functions for data exchange and launch tasks on device. The kernel corresponds to each such task.

- Thread - a data set to be processed,
- Warp is a group of 32 strands. Data is processed by warp,
- Block - a set of threads or warps,
- Grid - a set of blocks. All blocks organized in a grid have the same size and dimension.

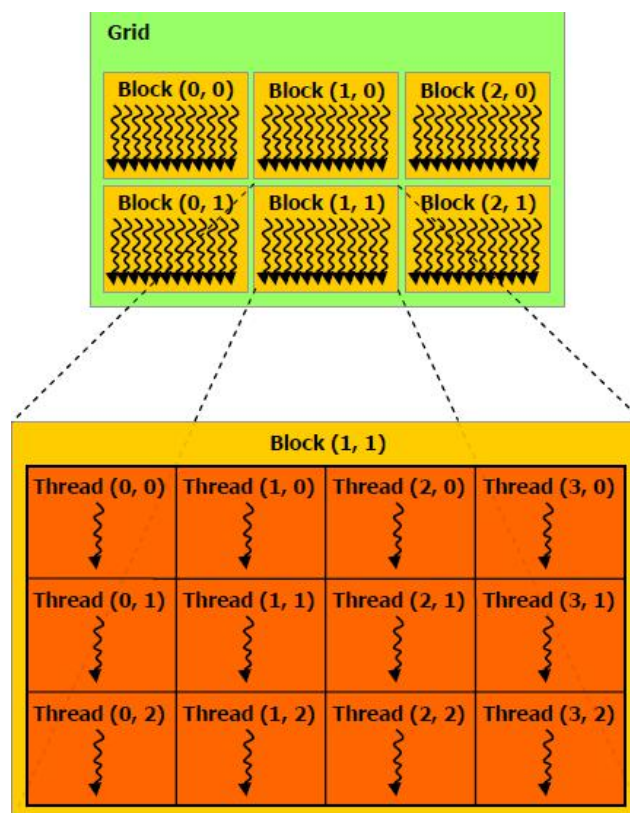


Fig. 2.1. Thread hierarchy in CUDA

This separation of data is used to improve productivity. Blocks are executed in parallel if the number of multiprocessors is large, otherwise data blocks are processed in series. Each subtask is executed by all threads in the block. The threads are combined into warps inside the block so that the threads belonging to different blocks cannot interact with each other.

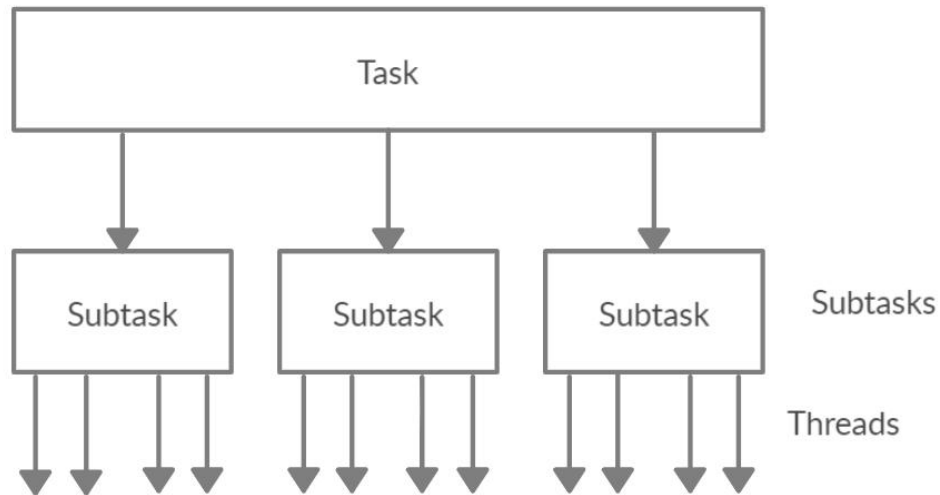


Fig. 2.2: Division of the initial task into a set of independently solved subtasks

2.1 NVidia Graphic Card Architecture

Consider the architecture of the GeForce 8800 GT graphics card.

The CPU communicates with the GPU through a special bridge. The chip consists of seven TPC (texture processor clusters), which, in turn, consists of two SM (streaming multiprocessors), a block of textures, a first level cache, and a combined texture cache. SM contains eight SP (streaming multiprocessors), also called CUDA kernels and two superfunction blocks SFU. Also SM structure includes a constant cache, a cache of instructions and the divided memory which provides communication of threads in one block.

A balance of parameters must be maintained, so NVIDIA recommends the use of blocks with 128 or 256 threads, as a block consisting of 512 threads has increased latency.

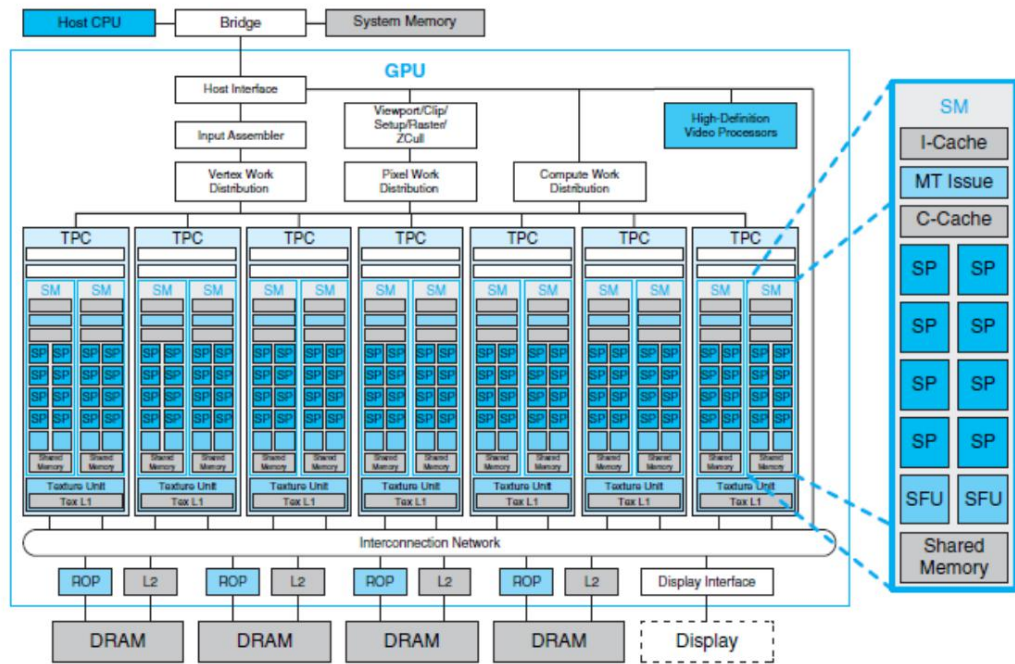


Fig. 2.3: GeForce 8800 GT Graphic Card Architecture

Chapter 3

Model Overview

Let us consider the biochemical process of hormone T_4 synthesis occurring in the thyroid follicle.

The first stage is the intake of iodine (I) into the follicular cells. Then, after the transition of iodine into an active state, it enters the colloid from epithelial cells with the help of special transport proteins. Free thyroglobulin (Tg), which is not associated with iodine yet, is stored in colloid. Thyroid hormones are formed when iodine is bound to thyroglobulin molecules. The storage of hormones in the thyroglobulin bonded form continues until the serum's T_4 level drops. In this case, the hormone is detached from thyroglobulin and enters the bloodstream from the thyrocyte.

In this work in the model the intensity of iodine penetration is proportional to the follicle surface area, i.e. actually the follicle contact area with the blood flow. The main characteristic of the model's work will be the dynamics of changes in the diameters of individual follicles.

3.1 Model Description

The follicle will be seen as a single chamber where colloid and thyrocytes are combined. However, all major processes that should take place in the follicle, such as the intake of active iodine, the addition of iodine to thyroglobulin, the formation of hormone, as well as the release of hormone through the wall of the chamber will be included in the model. Following [6], instead of the area, let us consider the expression $(\alpha D + \beta)$, where $\alpha = -0.015$, $\beta = 3.138$ and D is the follicle size.

The dimensions of normal follicles correspond to the lognormal distribution [6]:

$$f(x) = \frac{1}{\sqrt{2\pi}\sigma x} \exp\left[-\frac{(\ln x - \mu)^2}{2\sigma^2}\right] \quad (3.1)$$

Also in [10], a distribution of (3.1) for rat follicle sizes was obtained with parameters $\mu = 3.78$ and $\sigma = 0.305$ for central follicles, and parameters $\mu = 3.96$ and $\sigma = 0.52$ for peripheral follicles. The ratio of the central follicles to the peripheral follicles was 78% to 22%. However, in a number of pathologies, the follicle size distribution may shift to other distributions [10], e.g., the Relay distribution.

Also the penetration rate depends on the concentration of iodine in blood v and the difference in iodine concentration in the follicle u_l^0 .

The process of formation of the hormone T_4 will be described by a system of ordinary differential equations. Following the work [2], complicating the original system.

For this purpose it is necessary to enter the notation of substance concentrations in the chamber.

- u_I - concentration of iodine in the follicle,
- $u_{Tg}^{(1)}$ - concentration of iodized thyroglobulin,
- $u_{Tg}^{(2)}$ - concentration of unbound thyroglobulin,
- u_{T4} - the concentration of hormone T_4 .

$$\frac{1}{s} \frac{du_I}{dt} = (\alpha D + \beta)v(u_I^0 - u_I) - a_1 u_I \frac{u_{Tg}^{(2)}}{b_2 + u_{Tg}^{(2)}}, \quad (3.2)$$

$$\frac{1}{s} \frac{du_{Tg}^{(1)}}{dt} = \gamma a_1 u_I \frac{u_{Tg}^{(2)}}{b_2 + u_{Tg}^{(2)}} - a_2 u_{Tg}^{(1)} \frac{u_{T4}}{b_3 + u_{T4}}, \quad (3.3)$$

$$\frac{1}{s} \frac{du_{Tg}^{(2)}}{dt} = a_3(b_1 - v)u_{Tg}^{(2)}(H - u_{Tg}^{(2)}) - \gamma a_1 u_I \frac{u_{Tg}^{(2)}}{b_2 + u_{Tg}^{(2)}}, \quad (3.4)$$

$$\frac{1}{s} \frac{du_{T4}}{dt} = \delta a_2 u_{Tg}^{(1)} \frac{u_{T4}}{b_3 + u_{T4}} - P_{T4} u_{T4}, \quad (3.5)$$

where a_i, b_i, γ, δ are system parameters, P_{T4} is the rate of hormone T_4 elimination from the follicle. Parameter s characterizes the rate of chemical reactions.

Equation (2) describes the rate at which iodine enters the follicle (first summand) and the rate with which iodine decreases due to its binding to thyroglobulin (second summand).

Equation (3) describes the rate of change in thyroglobulin iodine-related content, which depends on the rate of thyroglobulin binding to iodine and the rate of formation of the hormone T_4 .

Equation (4) describes the rate of change in free thyroglobulin. The first summation describes the rate of free thyroglobulin formation by thyrocytes; the rate of formation is influenced by thyrotropin, the hormone produced by adenohypophysis. The amount of thyrotropine, in its turn, decreases with increasing the concentration of iodine in the blood v - multiplier $(b_1 - v)$. Due to the structure of the differential equation (Bernoulli's equation) [4] the maximum possible concentration of

thyroglobulin is H , and the minimum concentration is zero.

Equation (5) describes the rate of the hormone T_4 formation and its release into the bloodstream.

Colloid contains thyroglobulin, iodine and other proteins. Thus, the diameter of the individual follicle will change based on stimulating thyroid hormones and iodine concentrations:

$$D = d_1 (u_{Tg}^{(1)} + u_{Tg}^{(2)}) + d_2 u_I. \quad (3.6)$$

Here d_i are the ratios of proportionality between the follicle size and the i -th substance.

Let us consider the work of the thyroid gland containing N follicles. Let us assume that the follicle size is distributed by the lognormal law (3.1). Then we set the total concentration of iodine in the blood $V = \sum_{i=1}^N v_i$, where v_i is the iodine concentration of the i -th follicle. The iodine concentrations of v_i are evenly distributed among all follicles. In other words, v_i takes V/N values.

3.2 Computer Characteristics

All measurements were made on HP Gaming Pavilion - 15-cx0030ur.

Processor: Intel® Core™ i5+ 8300H

The characteristics of the craphic card:

Device name	GeForce GTX 1050 Ti
Total global memory	4096 Mb
Shared memory per block	49152
Registers per block	65536
Warp size	32
Multiprocessor count	6

Table 3.1: Characteristics of the graphic card

3.3 Data preparation

The first step in solving the system of ordinary differential equations is to determination of starting values of diameter and concentrations of all substances.

We generate the starting diameter according to the lognormal law, according to formula (1).

In C++ there is a built-in generator of values in the lognormal distribution:

```
void Diameter(float *D_0, int numOfFollicule)
{
    random_device rd;
    mt19937 gen(rd());
    lognormal_distribution<> X(3.78, 0.305);
    for (int i = 0; i < numOfFollicule; i++)
    {
        double k = X(gen);
        D_0[i] = k;
    }
}
```

where

- numOfFollicule is the number of follicles that we set;
- array D_0 stores generated starting diameters;
- random_device class is designed to generate a random sequence using an external device.

- mt19937 is a 32-bit pseudo-random generator of random number, the degree of "randomness" is quite high, based on the properties of prime numbers, high speed.

The lognormal_distribution of random numbers generates random numbers $x > 0$ according to the normal logarithmic distribution.

In the case of CUDA technology, there is also an integrated log-normal distribution generator, but there are several difficulties with its application.

1. Generation works slowly

When feeding follicle count is 100,000, the time taken to generate is approximately 980 milliseconds.

```
__global__ void Diameter(Base_Type *D_0, Base_Type *D_temp, int size,
                        Base_Type mu, Base_Type sig, int shift, int count, int key)
{
    curandState s1;
    int k = blockDim.x*blockIdx.x + threadIdx.x;
    curand_init(key, 0, k, &s1);
    if (k < count)
    {
        D_0[k + shift*size] = curand_log_normal(&s1, mu, sig);
        D_temp[k] = D_0[k + shift*size];
    }
}
```

For correct work of the generator you should use auxiliary functions, such as `curand_init()`. After some experiments, it was found out that most of the time is spent on it.

The `curand_init()` function sets the initial state assigned by the calling party using the specified initial number, sequence number and offset within the sequence. Different starting data guarantee different starting states and different sequences. The same data always produce the same state and the same sequence.

Calls of `Curand_init()` function are slower than `curand()` or `curand_uniform()` calls, but give more guarantees about the mathematical properties of the generated sequences.

`Curand_init()` is a heavy function, so to speed up the program, it must be separated into a separate kernel.


```

__global__ void curandInit(curandState *state, int key)
{
    int id = blockDim.x*blockIdx.x + threadIdx.x;
    curand_init(key, id, 0, &state[id]);
}

__global__ void diameter(Base_Type *D_0, Base_Type *D_temp, int size,
                        Base_Type mu, Base_Type sig, curandState *state, int shift, int count)
{
    int k = blockDim.x*blockIdx.x + threadIdx.x;
    if (k < count)
    {
        D_0[k + shift*size] = curand_log_normal(&state[k], mu, sig);
        D_temp[k] = D_0[k + shift*size];
    }
}

```

In this case, at 100,000 follicles, about 510 milliseconds are spent, of which 0-2 milliseconds are used to obtain the distribution.

2. It is also necessary to break down the number of follicles into several parts.

If the number of follicles exceeds 180,000 when `curand_init()` is executed in `diameter()` kernel and 260,000 when `curand_init()` is selected in a separate kernel, no values are generated.

The graph below shows the dependence of the generator running time on changes in the critical value of the number of follicles.

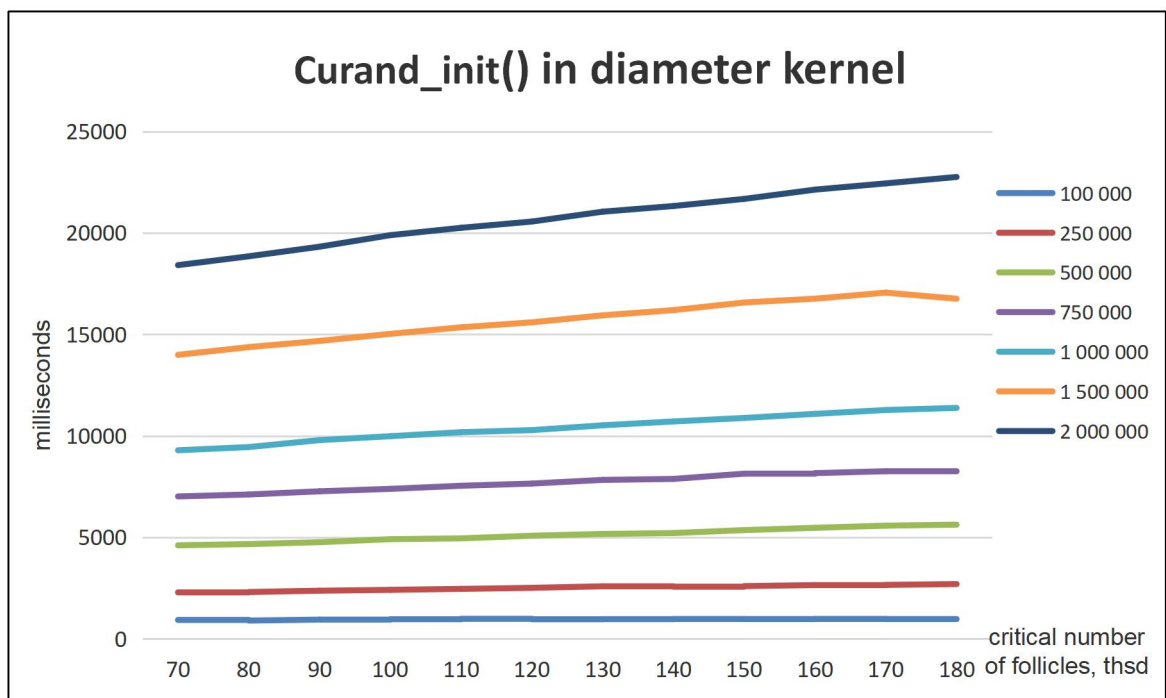


Fig. 3.1: Diameter Generation in one kernel

Next, let's consider the graph of dependence of the generator running time on changing the critical value of the number of follicles, where the kernel filling the array of states is taken separately.

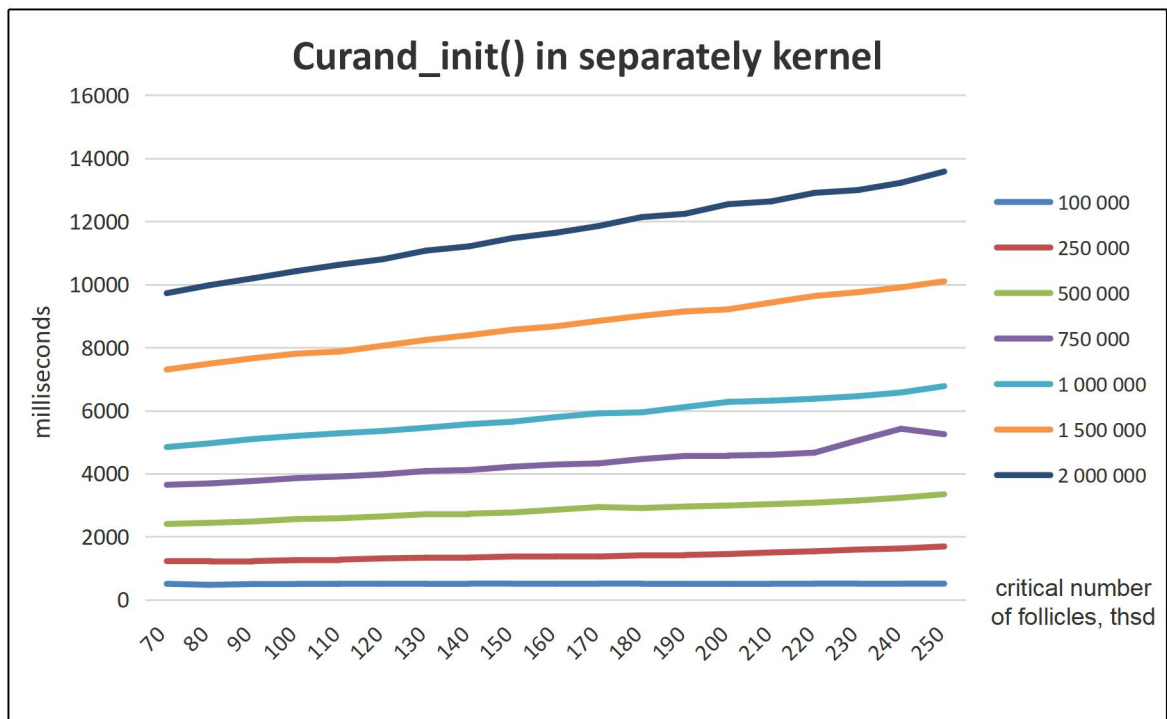


Fig. 3.2: Diameter Generation With Separately Curand_init() Kernel

In both cases, you can see that by dividing the number of follicles into smaller parts, you can significantly reduce the running time of the generator. Also when charts compare, the theory proves that acceleration also occurs when curand_init() is separated into a separate kernel.

Let's compare the running time of all versions of generators, the critical value for the partition, when using CUDA, fix as critical = 100,000.

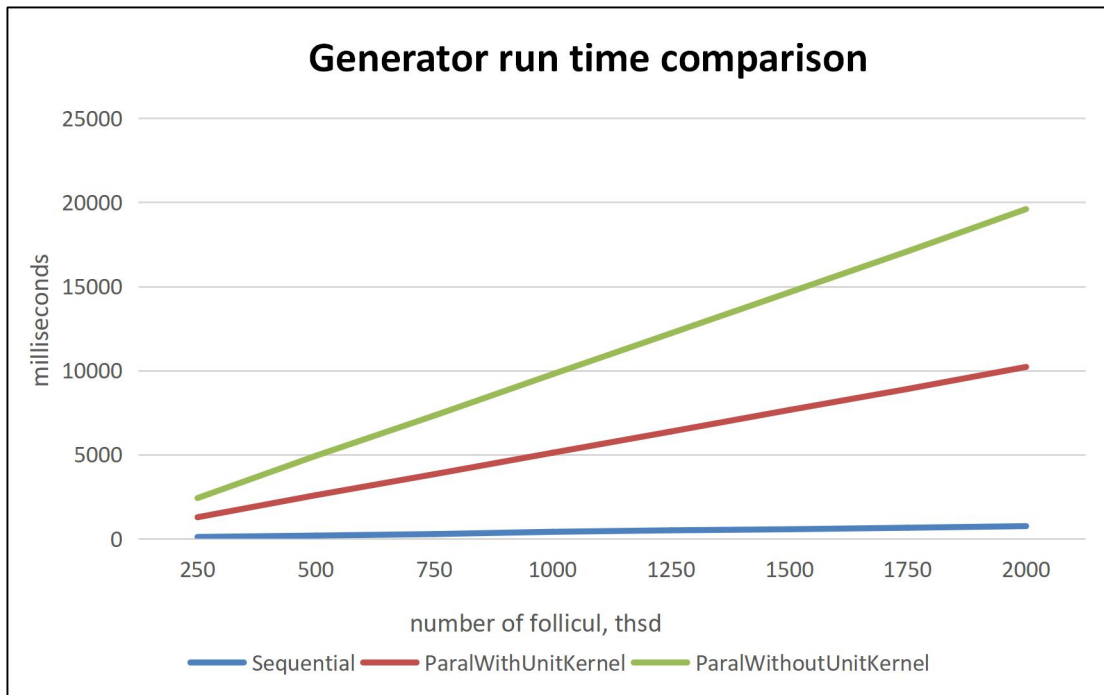


Fig. 3.3: Time Comparison

The C++ generator allows you to generate a sequence distributed by log-normal law much faster.

The chart below shows the initial diameter distribution at $N = 100,000$.

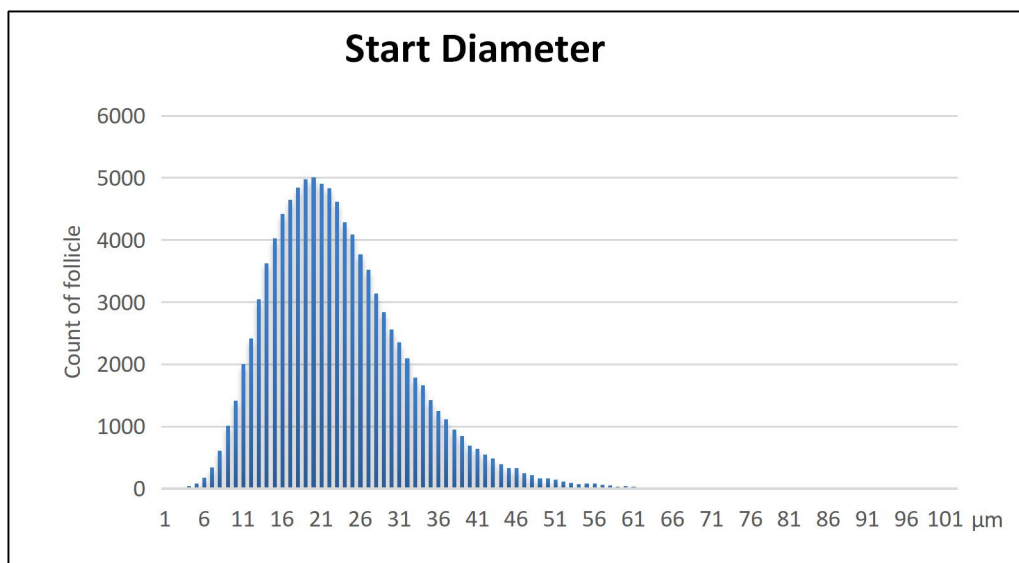


Fig. 3.4: Start Diameter

After receiving all diameters, it is necessary to calculate the initial concentration of all substances in the follicle. The starting values are taken from [2], but in this work they depend on the diameter of the i -th follicle:

```

__global__ void startValues(Base_Type *D_0, int size, Base_Type *u_I_0,
Base_Type *u_Tg_Free_0, Base_Type *u_Tg_lod_0, Base_Type *u_T4_0)
{
    int k = blockDim.x*blockIdx.x + threadIdx.x;
    if (k < size)
    {
        u_I_0[k] = 0.04 * D_0[k] / 45;
        u_Tg_Free_0[k] = 1.2 * 0.5 * D_0[k] / 45;
        u_Tg_lod_0[k] = 1.2 * 0.5 * D_0[k] / 45;
        u_T4_0[k] = 1.0 * D_0[k] / 45;
    }
}

```

To solve the system of ordinary differential equations, two methods were chosen to compare the speed and accuracy of calculations.

3.4 Euler's method

This method is the simplest method for calculating differential equations. It is a one-step method with first order accuracy. The accuracy of calculation changes relatively to the step linearly, i.e. when the step is halved, the accuracy will also double.

Each thread is calculated in parallel and independently.

```

void Euler()
{
    if (k < numOfFollicule)
    {
        Base_Type h = 1.0 / CountOfMeasurements;

        for (int i = 0; i < CountOfMeasurements - 1; i++)
        {
            I_new = I_start + du_I()*h;
            Tg_lod_new = Tg_lod_start + du_Tg_lod()*h;
            Tg_Free_new = Tg_Free_start + du_Tg_Free()*h;
            T4_new = T4_start + du_T4()*h;
            Diam_new = du_Diam(I_new, Tg_lod_new + Tg_Free_new);

            I_start = I_new;
            Tg_lod_start = Tg_lod_new;
            Tg_Free_start = Tg_Free_new;
            T4_start = T4_new;
            Diam_start = Diam_new;
        }
    }
}

```

Let us consider cases of iodine excess and deficiency to estimate the general dynamics of follicle diameters.

3.4.1 Results

- Express iodine

At uniform distribution of iodine at each iteration on all follicles $v_i = 0.96$ the sizes of follicles have a tendency to decrease. It indicates excess of iodine. By the twentieth day, the size distribution is visually similar to the geometric distribution.

The graphs below illustrate the change in overall diameter dynamics every five days.

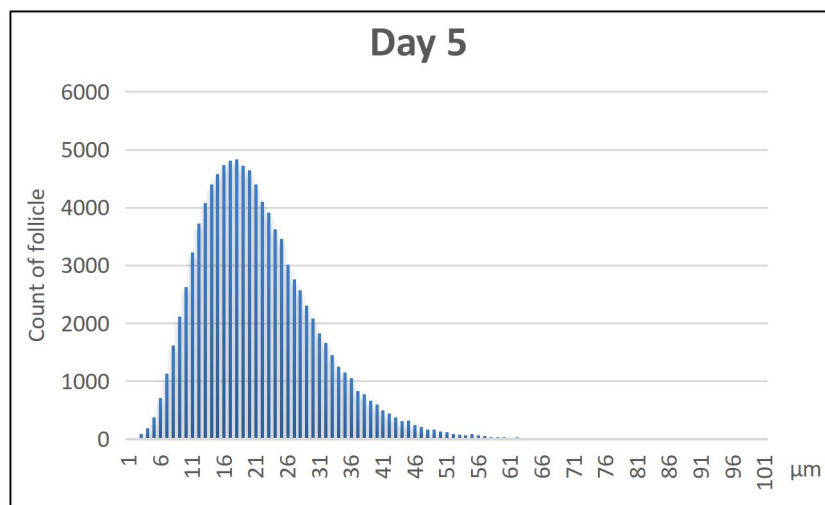


Fig. 3.5: Express iodine day 5

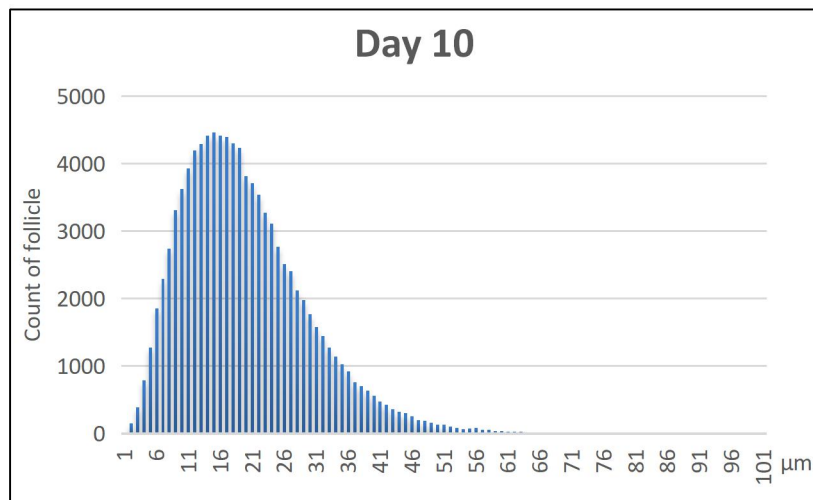


Fig. 3.6: Express iodine day 10

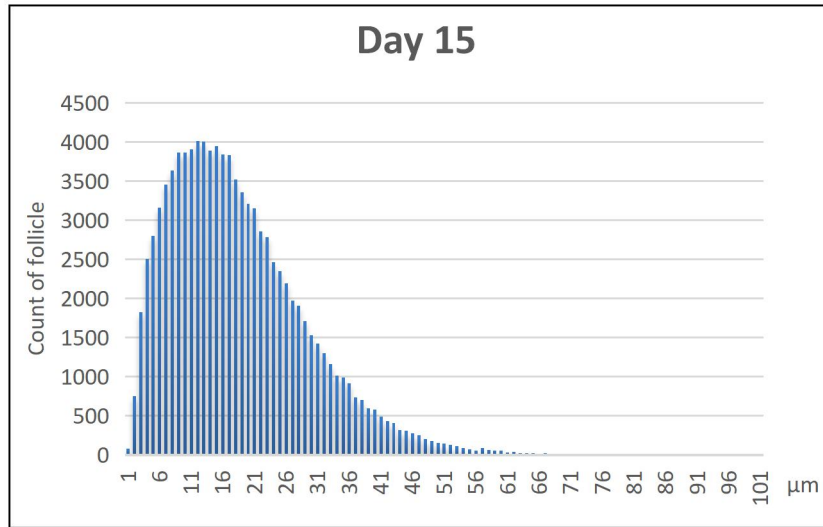


Fig. 3.7: Express iodine day 15

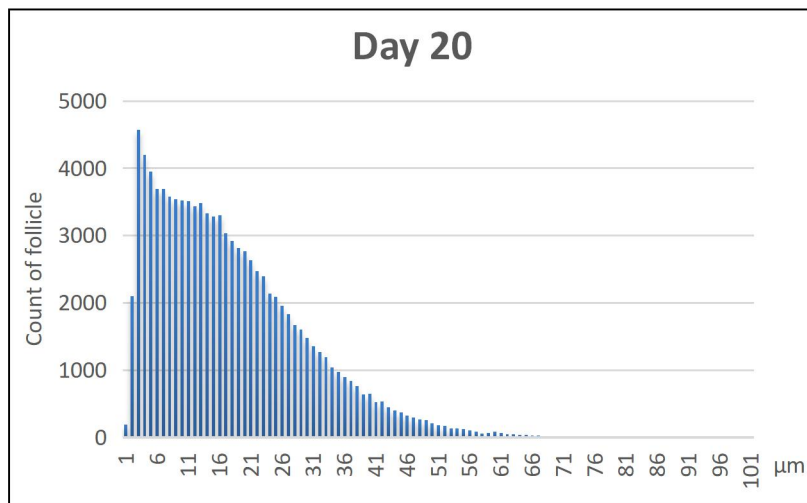


Fig. 3.8: Express iodine day 25

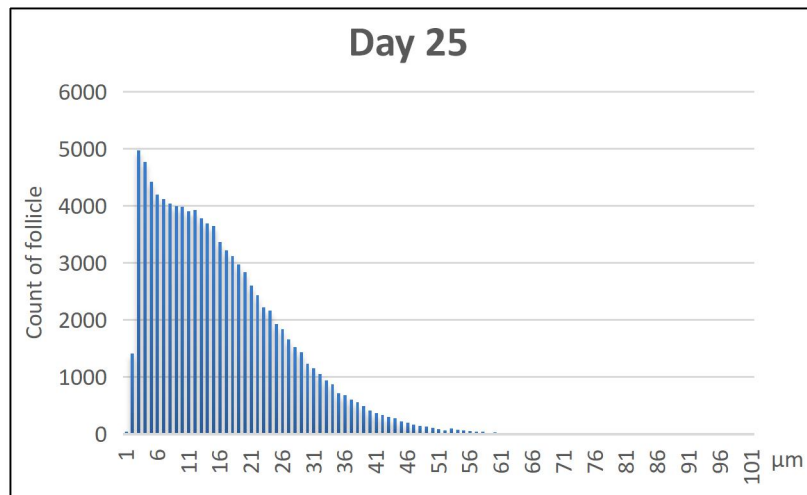


Fig. 3.9: Express iodine day 25

- Iodine deficiency

With iodine deficiency, the diameters gradually increase in size, in case of thyroid hormones are accumulated in themselves.

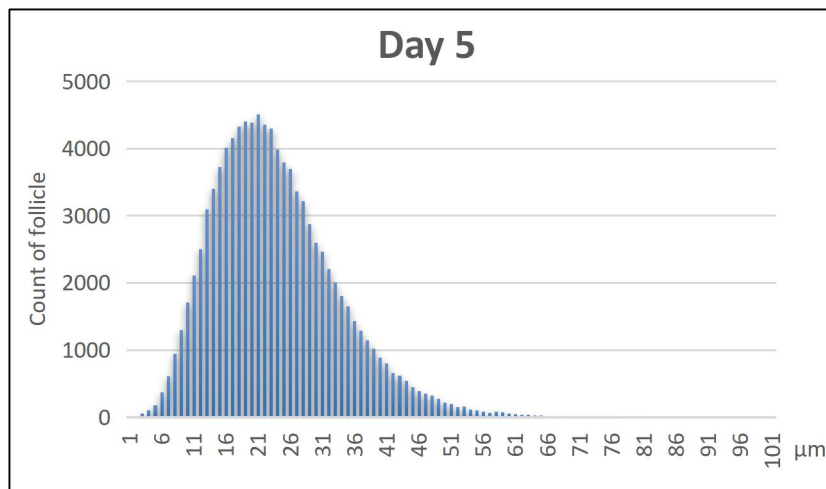


Fig. 3.10: Iodine deficiency day 5

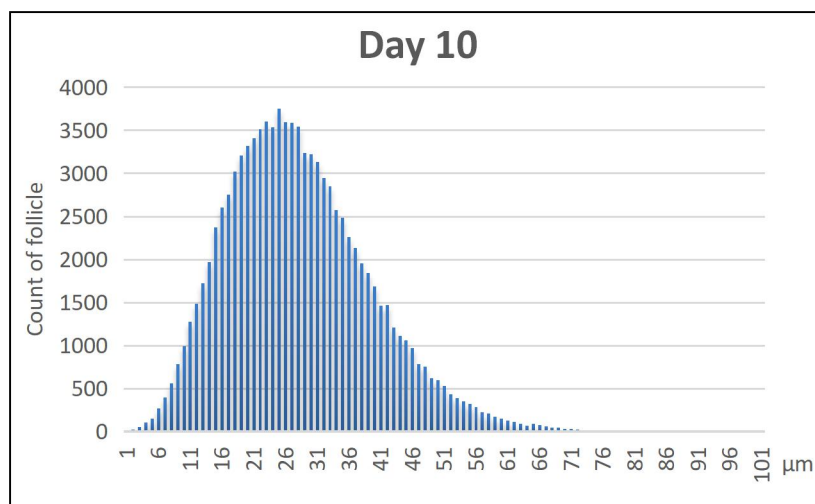


Fig. 3.11: Iodine deficiency day 10

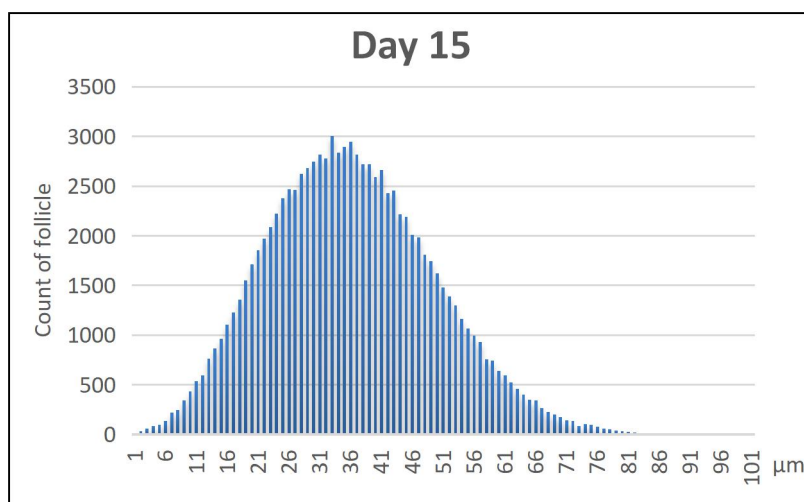


Fig. 3.12: Iodine deficiency day 15

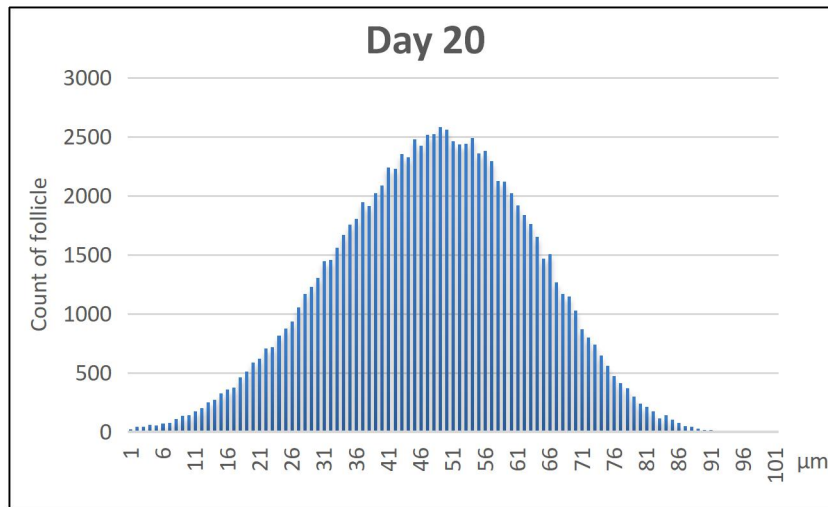


Fig. 3.13: Iodine deficiency day 20

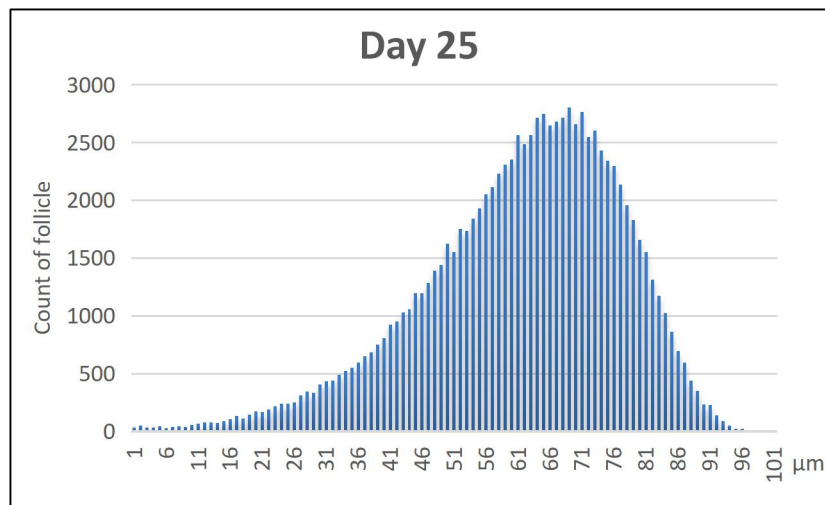


Fig. 3.14: Iodine deficiency day 25

The above charts show that when iodine collocation = 0.92, a thyroid hormone accumulates inside the colloid, thus provoking an increase in the size of each follicle. This indicates iodine deficiency

3.5 Runge-Kutta method

In the classical version, the accuracy of the method is $O^4(h)$. This method is used in practice most often because it combines high accuracy and performance.

However, the Runge-Kutta method is a serial algorithm, so, as in the Euler method, the function is calculated independently for each follicle, and the method is not paralyzed:


```

__global__ void RungeKutta()
{
    int k = blockDim.x * blockIdx.x + threadIdx.x;
    if (k < numOfFollicule)
    {
        Base_Type I_start = u_I_0[k], I_new;
        Base_Type Tg_lod_start = u_Tg_lod_0[k], Tg_lod_new;
        Base_Type Tg_Free_start = u_Tg_Free_0[k], Tg_Free_new;
        Base_Type T4_start = u_T4_0[k], T4_new;
        Base_Type Diam_start = Diam[k], Diam_new;
        Base_Type h = 1.0 / CountOfMeasurements;

        Base_Type k1_I, k2_I, k3_I, k4_I;

        ...

        for (int i = 0; i < CountOfMeasurements - 1; i++)
        {
            k1_I = du_I(V_i[k], I_start, Tg_Free_start, T4_start, Diam_start)*h;
            k1_Tg_lod = du_Tg_lod(I_start, Tg_Free_start, Tg_lod_start, T4_start)*h;
            k1_TgFree = du_Tg_Free(V_i[k], I_start, Tg_Free_start, T4_start)*h;
            k1_T4 = du_T4(I_start, Tg_lod_start, T4_start)*h;

            ...

            k4_I = du_I(V_i[k], I_start + k3_I, Tg_Free_start + k3_TgFree, T4_start + k3_T4, Diam_start + h)*h;
            k4_Tg_lod = du_Tg_lod(I_start + k3_I, Tg_Free_start + k3_TgFree, Tg_lod_start + k3_Tg_lod, T4_start + k3_T4)*h;
            k4_TgFree = du_Tg_Free(V_i[k], I_start + k3_I, Tg_Free_start + k3_TgFree, T4_start + k3_T4)*h;
            k4_T4 = du_T4(I_start + k3_I, Tg_lod_start + k3_Tg_lod, T4_start + k3_T4)*h;

            I_new = I_start + (k1_I + 2 * k2_I + 2 * k3_I + k4_I) / 6.0;
            Tg_lod_new = Tg_lod_start + (k1_Tg_lod + 2 * k2_Tg_lod + 2 * k3_Tg_lod + k4_Tg_lod) / 6.0;
            Tg_Free_new = Tg_Free_start + (k1_TgFree + 2 * k2_TgFree + 2 * k3_TgFree + k4_TgFree) / 6.0;
            T4_new = T4_start + (k1_T4 + 2 * k2_T4 + 2 * k3_T4 + k4_T4) / 6.0;
            Diam_new = du_Diam(I_new, Tg_lod_new + Tg_Free_new);

            I_start = I_new;
            Tg_lod_start = Tg_lod_new;
            Tg_Free_start = Tg_Free_new;
            T4_start = T4_new;
            Diam_start = Diam_new;
        }
        u_I_0[k] = I_new; u_Tg_lod_0[k] = Tg_lod_new;
        u_Tg_Free_0[k] = Tg_Free_new; u_T4_0[k] = T4_new; Diam[k] = Diam_new;
    }
}

```

3.5.1 Results

- Express iodine

According to the diagrams of the fifth and twenty-fifth days, we can conclude that the overall dynamics of follicle size change shifts in the same way as with the Euler method.

$I = 0.96$.

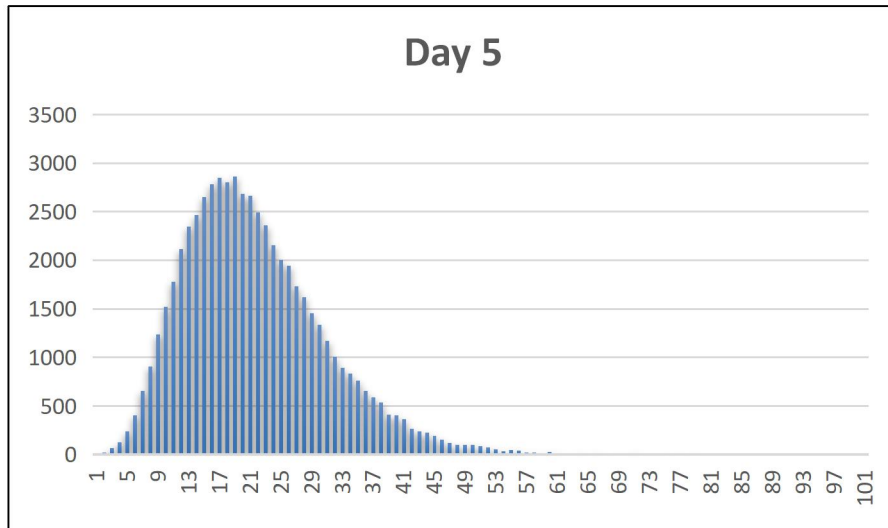


Fig. 3.15: Express iodine day 5

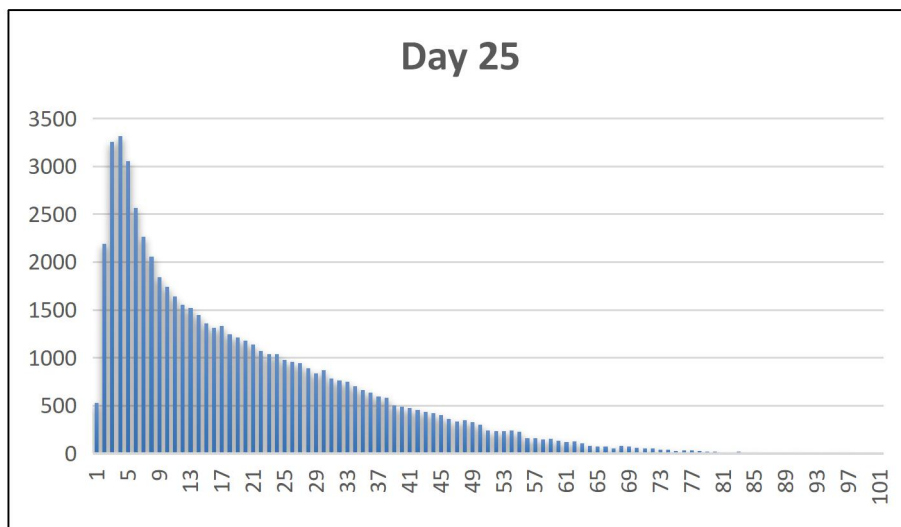


Fig. 3.16: Express iodine day 25

- Iodine deficiency

With iodine deficiency there is a tendency to increase all diameters and to accumulate iodine-containing hormones inside the follicle.

$$I = 0.92$$

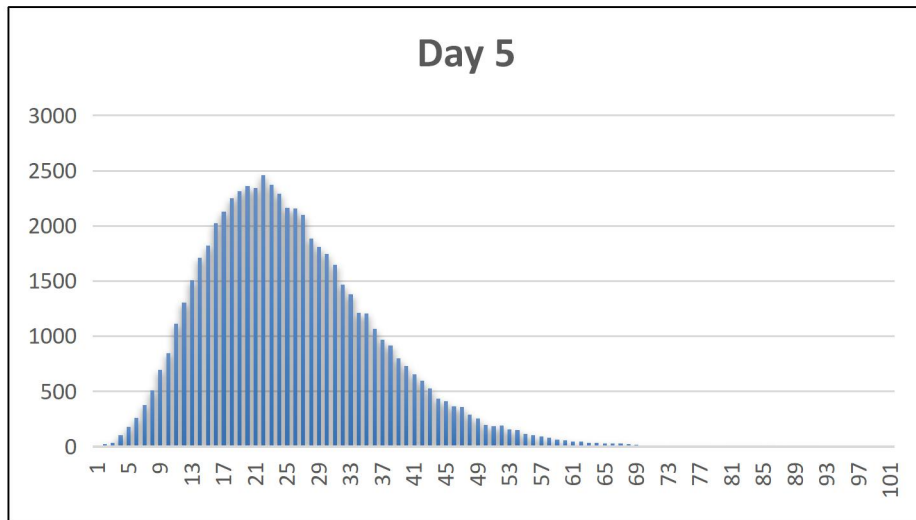


Fig. 3.17: Iodine deficiency day 5

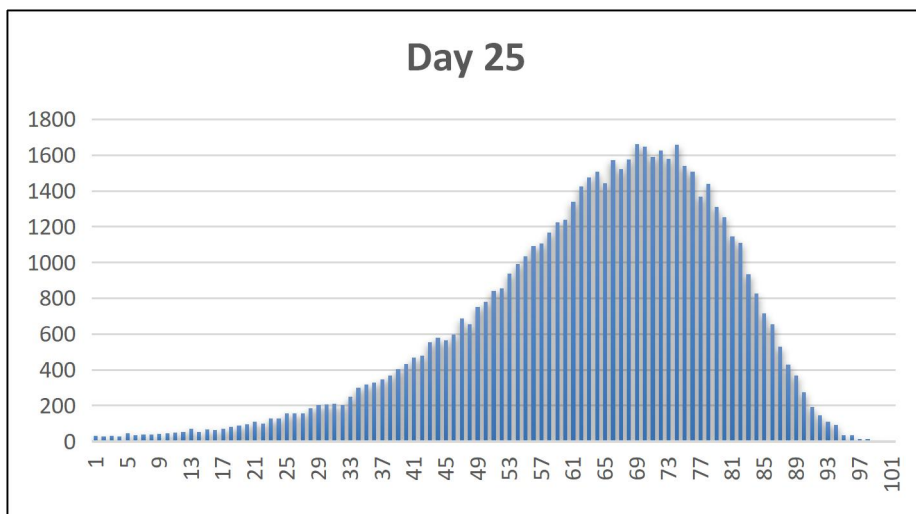


Fig. 3.18: Iodine deficiency day 25

3.6 Comparison of methods

It is necessary to compare two methods. To check how qualitatively and quickly calculation of systems of the ordinary differential equations at use of technology CUDA is carried out.

3.6.1 Accuracy of calculations

For more convenience, quality control methods should be fixed $I = 0.96$, we also take for calculation the number of follicles = 100 000.

Here are the graphs of follicle size dynamics at excess iodine using both methods to compare the accuracy of calculations.

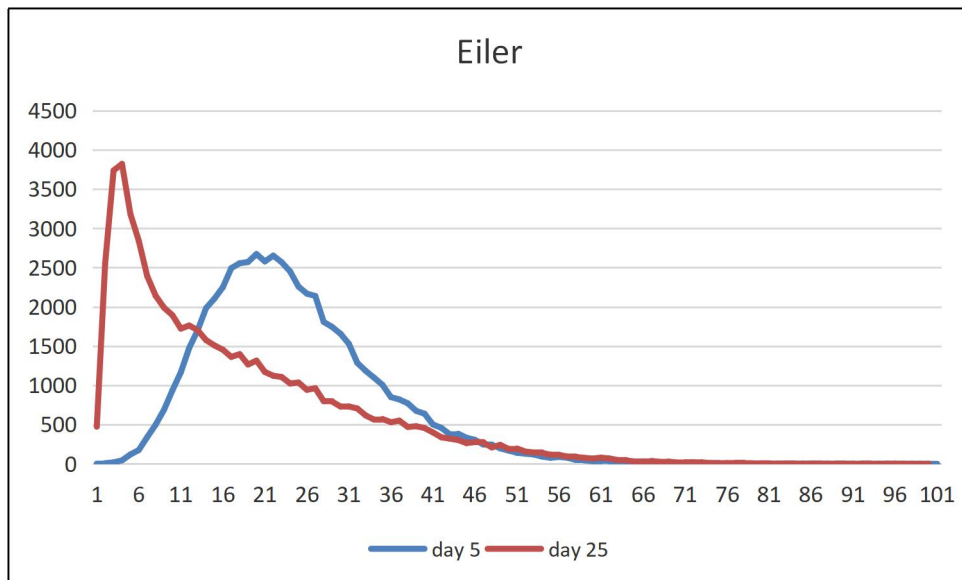


Fig. 3.19: Diameter size with Euler Method

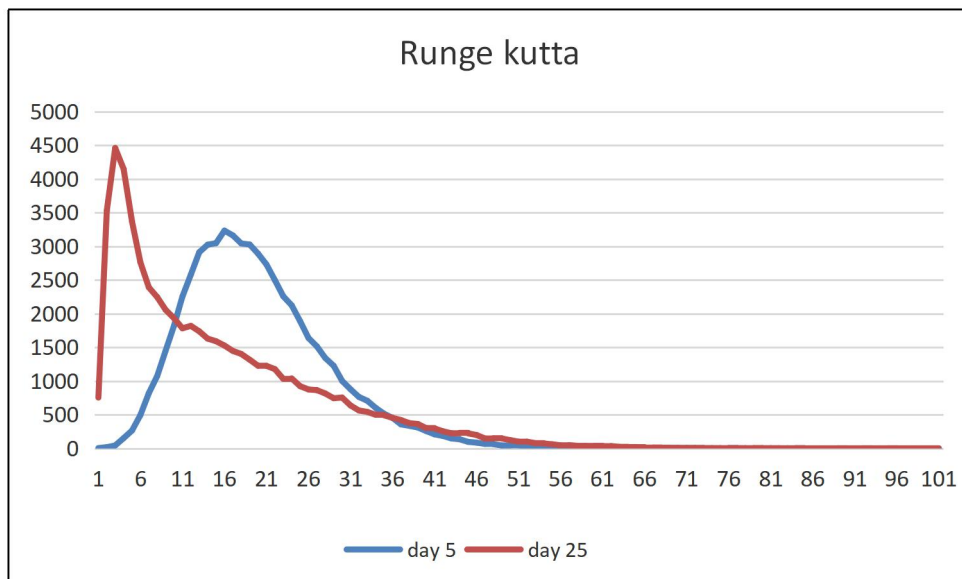


Fig. 3.20: Diameter size with Runge-Kutta Method

The above charts show the mixing of follicle diameters with excess iodine. At comparison of corresponding days on the schedule fluctuations in size are more clearly traced solving by the Euler method, than solving by the Runge-Kutta method.

3.6.2 Speed of work

When measuring speed for comparison, it is necessary to take parallel and sequentially implemented methods.

The speed is calculated in milliseconds, two methods are compared using C++ and CUDA.

Number Of Follicle	Sequential Euler method, ms	Parallel Euler method, ms	Sequential Runge-Kutta method, ms	Parallel Runge-Kutta method, ms
100 000	4378	202	15625	1822
200 000	8809	409	31034	3652
300 000	13680	614	45962	5498
400 000	17391	828	61314	7371
500 000	21556	1043	76755	9836
600 000	26134	1262	91086	11063
700 000	27944	1475	106234	12893
800 000	31190	1682	121629	14723
900 000	34900	1898	139616	16729
1 000 000	35973	2124	156940	18570
1 100 000	39138	2338	173064	20438
1 200 000	42889	2553	188432	22338
1 300 000	46437	2772	203325	24332
1 400 000	49899	2983	216314	26201
1 500 000	53500	3197	234945	28084
1 600 000	56969	3416	350569	29937
1 700 000	61241	3632	264304	32807
1 800 000	65133	3844	281045	33680
1 900 000	68748	4059	297839	35548
2 000 000	72281	4273	313017	37461

Table 3.2: Method speed

Compared to the Euler method realized using CUDA, the parallel version of method Runge-Kutta works on the average 8.835 times faster. Moreover at when comparing the dynamics of changes in the size of the follicles, the error of the Euler method is insignificant.

However, there are situations when accuracy is important. Despite the fact that the Runge-Kutt method does not parallel, when solving a huge number of systems, it is possible to achieve an average acceleration of 8.34 times.

3.7 Withdrawal

At construction of model there were some difficulties, such as:

- When using CUDA technology, no sequence of starting diameters was generated if the number of follicles exceeded 180,000.

- The parallel version generator is slow, time increases linearly when the number of follicles increases from 100,000 to 2,000,000.

One of the solutions is to separate `curand_init()` into a separate kernel for maximum acceleration of parallel generation of starting diameters. It is also possible to use the built-in C++ generator for generating a sequence by log-normal distribution when the number of follicles is up to 2 000 000.

When using `curand_init()`, divide arrays into smaller ones and call them in the loop to fill all necessary values.

Cases of iodine excess and deficiency have been considered:

- With constant iodine deficiency follicles "inflate", accumulating iodine-containing hormones.

- In a situation of iodine deficiency follicle diameters tend to reduce, producing a huge number of thyroid hormones.

comparison of the two methods for solving the ODU system led to the conclusion, that with a large amount of data is more profitable to use the technology CUDA. Moreover, the accuracy of the Runge-Kutt method does not strongly influence the overall diameter dynamics, which suggests that the simpler and faster Euler method is best suited for this model.

Conclusion

The main results of the dissertation are as follows:

- 1 Materials and articles on modeling the thyroid gland were studied in this dissertation.
- 2 A model of a single follicle was constructed with the scientist changing the follicle diameter, which depends on the concentration of incoming iodine.
- 3 The number of follicles for modeling the entire thyroid gland has been increased.
- 4 The speed and efficiency of methods for solving the system of ordinary differential equations are studied.
- 5 CUDA technology was used to accelerate the work.
- 6 The comparative analysis of the serial and parallel versions of programs was carried out.

The main objective of the work was to create a model that simulates thyroid function at the follicle level. The behavior of the parameter responsible for follicle size was analyzed.

- 1 On the basis of the studied materials, a model showing the thyroid response to excess and deficiency of incoming iodine was constructed.
- 2 Two methods for comparing the quality of calculations and the speed of work were chosen for the solution of the TEM system.
- 3 In the course of the work, schedules were built to check the model and visualize the results obtained. This allowed facilitating the analysis of the program's work.
- 4 In the course of the study it was also checked how beneficial it is to use GPU when calculating the system on a large number of follicles. Moreover, conclusions were made as to how expedient it is to use the generator of a sequence distributed by log-normal law.

Thus, a mathematical model of the thyroid gland was constructed, considering the thyroid gland as a mega-system consisting of a certain number of follicles. According to the results of the study, this approach allows To track changes occurring in the individual follicle more accurately. The

size distribution changes relatively logarithmically up or down separately. The construction of charts allows you to determine how much iodine was applied to the input. If there is not enough iodine, the sizes of individual follicles tend to increase, if there is excess, on the contrary, to decrease. This study allows you to adjust the daily intake of iodine to stabilize the size of the thyroid gland, thereby avoiding deviations in its work.

For quick calculation of sizes it is better to combine serial and parallel versions of programs. It will be time-saving to combine serial generation of the starting set of follicle sizes with parallel calculation of the system by the Euler method.

Bibliography

- [1] Anatomia and physiology in 2 volumes. volume 1 organism of man, his regulatory and integrative systems. Available at:
[https://studme.org/303277/meditsina/stroenie_funktsii_razvitie_zhelez_vnutrenney_sekretsii] (in Russian)
- [2] **Balykina H, Kolpak E, Kotina E.** Mathematical Model of Thyroid Function. Middle-East Journal of Scientific Research 19 (3): 429-433 (2014)
- [3] **Degon M., Chipkin S.R., Hollot C.V., R. Thomas Zoeller f, Yossi Chait.** A computational model of the human thyroid. Mathematical Biosciences 212 (2008) pp. 22–53.
- [4] **Dror, A.A., etc.:** Atrophic thyroid follicles and inner ear defects reminiscent of cochlear hypothyroidism in Slc26a4-related deafness. Mamm. Genome 25(7-8), 304-16 (2014).
- [5] **Hartoft-Nielsen M. L., Rasmussen Å. K., Feldt-Rasmussen U., Buschard K. and Bock T.** Blackwell Publishing, Ltd. Estimation of number of follicles, volume of colloid and inner follicular surface area in the thyroid gland of rats. J. Anat. (2005) 207, pp117–124
- [6] **Igbokwe, C. O., Ezeasor, D. N.:** Histologic and ultrastructural observations on the thyroid gland of the White Fulani (Zebu) cattle in Northern Nigeria. Afr. J. Biotechnol. 14(2), 156-166 (2015).
- [7] **Jackson, J.L.:** The shape and size of the human thyroid follicle in health and disease. Anat. Rec. 48(2), 219-239 (1931).
- [8] **Jairo Gomes da Silva, Rafael Martins de Moraes, Izabel Cristina Rodrigues da Silva, Paulo Fernando de Arruda Mancera.** Mathematical models applied to thyroid cancer. Biophysical Reviews (2019) 11. pp. 183–189.
- [9] **Jyoti R. Gaikwad, Santoshkumar A. Dope, Deepak S. Joshi.** Histogenesis of Developing Human Thyroid. Indian Medical Gazette, 2012. pp. 57-61
- [10] **Knigge, K.M.:** Influence of cold exposure upon the endocrine glands of the hamster, with an apparent dichotomy between morphological and functional response of the thyroid. Anat. Rec. 127(1), 75-95 (1957).
- [11] Mathematical Modeling of the Pituitary–Thyroid Feedback Loop: Role of a TSH-T3-Shunt and Sensitivity Analysis. Available at:
[<https://www.ncbi.nlm.nih.gov/pmc/articles/PMC5871688/>].

[12] Mathematical Modeling of Thyroid Size and Hypothyroidism in Hashimoto's Thyroiditis Balamurugan Pandiyan. Available at: [<https://www.intechopen.com/books/goiter-causes-and-treatment/mathematical-modeling-of-thyroid-size-and-hypothyroidism-in-hashimoto-s-thyroiditis>]

[13] Ministry of Health of the Russian Federation. Statistical Collection 2014. Available at: [<https://www.rosminzdrav.ru/ministry/61/22/stranitsa-979/statisticheskie-i-informatsionnye-materialy/statisticheskiy-sbornik-2014-god>] (in Russian)

[14] Ministry of Health of the Russian Federation. Statistical Collection 2017. Available at: [<https://www.rosminzdrav.ru/ministry/61/22/stranitsa-979/statisticheskie-i-informatsionnye-materialy/statisticheskiy-sbornik-2017-god>] (in Russian)

[15] **Ognerubov N., Zhukov A., Sergeev R.** Individual differences of surgery anatomy of thyroid gland: literature review. Bulletin of Russian universities. Mathematics. 2016. №2, pp. 520-529. (in Russian)
<https://cyberleninka.ru/article/n/individualnye-osobennosti-hirurgicheskoy-anatomii-schitovidnoy-zhelezy-obzor-literatury>

[16] **Sapin, Nikolenko, Nikityuk:** Human anatomy. Textbook. In 2 volumes. Volume 2, 2018, pp. 90-95. (in Russian)

[17] **Singh R. and Beigh S. A.** Diseases of Thyroid in Animals and Their Management. Insights from Veterinary Medicine, Rita Payan-Carreira, IntechOpen, February, 2013. DOI: 10.5772/55377. Available in: [<https://www.intechopen.com/books/insights-from-veterinary-medicine/diseases-of-thyroid-in-animals-and-their-management>]

[18] **Tomonari, M.:** Histological studies on the mammalian thyroid glands. Archivum Histol. Jap. 4, 497-523 (1959).

[19] **Yocom, H.B.:** Histological differences in the thyroid glands from two subspecies of *Peromyscus maniculatus*. Anat. Rec. 39(1), 57-67 (1928).